*Ecology*, 99(11), 2018, pp. 2506–2514


# Tree water balance drives temperate forest responses to drought

A. B. Berdanier[1,2,4] and J. S. Clark[2,3]

[1]*University Program in Ecology, Duke University, Durham, North Carolina 27708 USA*
[2]*Nicholas School of the Environment, Duke University, Durham, North Carolina 27708 USA*
[3]*Department of Statistical Science, Duke University, Durham, North Carolina 27708 USA*

*Abstract.* Intensifying drought is increasingly linked to global forest diebacks. Improved understanding of drought impacts on individual trees has provided limited insight into drought vulnerability in part because tree moisture access and depletion is difficult to quantify. In forests, moisture reservoir depletion occurs through water use by the trees themselves. Here, we show that drought impacts on tree fitness and demographic performance can be predicted by tracking the moisture reservoir available to trees as a mass balance, estimated in a hierarchical state-space framework. We apply this model to multiple seasonal droughts with tree transpiration measurements to demonstrate how species and size differences modulate moisture availability across landscapes. The depletion of individual moisture reservoirs can be tracked over the course of droughts and linked to biomass growth and reproductive output. This mass balance approach can predict individual moisture deficit, tree demographic performance, and drought vulnerability throughout forest stands based on measurements from a sample of trees.

*Key words:* *drought; ecophysiology; forest; growth; sap flux; soil moisture; tree; water balance.*

## Introduction

Anticipating the ecological consequences of drought (Allen et al. 2010, Clark et al. 2016) requires a capacity to predict drought-induced stress from moisture supply to forest stands (McDowell et al. 2011, Allen et al. 2015). Recent physiological studies clarify how drought stress varies among trees, species, and environments (e.g., Choat et al. 2012, Bennett et al. 2015). A critical metric of drought vulnerability for trees is the reservoir of water that trees can access (Vose et al. 2016). However, even when observations of root depth or distribution are available (Meinzer et al. 1999, Stahl et al. 2013), many studies rely on generalizations of the moisture reservoir capacity of individual trees and how it is depleted across landscapes. Improved estimates of this moisture reservoir and the variables that control it could enhance our understanding of drought stress and advance efforts to predict the physiological and demographic responses of temperate forests to changed environmental conditions (Vose et al. 2016).

The water available to individual trees is not easily tracked. During drought, soil moisture probes often report static values near the wilting point despite continued transpiration, as documented by sap flux data (Meinzer et al. 2013). This discrepancy can occur because the moisture reservoir accessed by roots is not captured by a small number of soil probes and without detailed measurements of root profiles. Landscape approaches, like microwave remote sensing, only quantify moisture in the upper soil surface (Jackson et al. 1996) and are not directly observed at the individual scale. The translation from precipitation arriving at the forest floor to a reservoir available for a given tree, as represented in many process models, would require knowledge of the three-dimensional rooting structure and soil porosity. Absent that information, researchers often assume average rooting distributions (e.g., Oren et al. 1998, Feng et al. 2014) or estimate individual rooting depth with isotope analysis (e.g., Stahl et al. 2013, Matheny et al. 2017), which are still a simplification of belowground structures and moisture access (Casper et al. 2003). Unlike canopy architecture, which provides strong evidence for light availability aboveground, the mass of belowground moisture available to individual trees remains largely unknown (Richter and Billings 2015).

Here, we use a mass balance approach paired with data on water use from sap flux measurements to estimate the potential reservoir controlled by each individual, how it is depleted, and how both are affected by tree size, species, and landscape position. We hypothesize that (1) the volume of individual tree moisture reservoirs can be predicted with basic individual-scale measurements and (2) there is a connection between reservoir depletion and the maintenance of important physiological and demographic processes. First, we examine the ability of the mass balance model to predict declines in sap flux during droughts. Across trees, we expect the mass balance to predict sap flux declines through time. Within trees, we expect estimates to be similar across multiple droughts. Next, we evaluate how reservoir depletion relates to loss of conductance and how deficits below potential transpiration relate to declines in growth and reproductive output to demonstrate consistency between model estimates and ecophysiological observations. Finally, we explore the drought responses of trees throughout a forest stand by predicting reservoir capacity and depletion during a drought. We expect aggregate measures of reservoir depletion and transpiration deficits to be comparable to other landscape-scale measurements. Additionally, we use these predictions to examine differences in the moisture reservoir and how it is depleted across species, sizes, and space. If the model estimates the individual reservoirs and predicts the

Manuscript received 21 June 2017; revised 13 July 2018; accepted 20 July 2018. Corresponding Editor: Paul B. Conn.
[4] E-mail: aaron.berdanier@gmail.com

progress of drought, then there is potential to understand forest responses to drought and identify the trees that are most susceptible to drought events with a mass balance.

## Methods

### *Tree water balance model*

We model the moisture reservoir for individual trees with a water balance. On a volume or mass basis, soil moisture depletion is the difference between inputs from precipitation ($P$) and losses from transpiration ($T$), evaporation ($E$), and gravitational outflows ($O$)

$$dS/dt = P(t) - O(t) - E(t) - T(t) \quad (1)$$

where $S$ is soil water storage. An assumption of average rooting depth for the forest stand is often used to place all variables in Eq. 1 on a common scale of volume or mass per ground surface area per time (Wilson et al. 2001). However, sap flux data show large heterogeneity between individuals, even within species and size classes (Berdanier et al. 2016), consistent with the known complexity of root architecture and soil structure (Cruiziat et al. 2002). This heterogeneity is responsible for differential impacts across landscapes, including tree death and morbidity (Berdanier and Clark 2016*a*).

Consider a landscape where trees each have access to a water reservoir $S_{i,t}$ (kg) determined by rooting architecture and moisture content. The dynamic reservoir varies among trees $i$ and over time $t$ due to size, landscape position, and species. The reservoir is equal to the potential reservoir $\omega_i$ (kg) for that individual under its current stand composition when soils are fully recharged. Recharge can occur before the onset of the growing season or after major rain events, although soils do not always reach field capacity (Appendix S2: Fig. S1). On any given day, the change in the reservoir state $S_{i,t}$ depends on the incoming precipitation and decreases due to runoff and drainage, evaporation, and transpiration, changing at a rate given by Eq. 1.

We used cumulative transpiration during drought to estimate the potential reservoir and how much of it remains at a given time. We assumed that during drought, the first three terms on the right-hand side of Eq. 1 are small, so moisture depletion for individual trees during drought is dominated by transpiration, and sap flux data can be used within a hierarchical state-space framework to estimate dynamic transpiration losses (Bell et al. 2015). The first point simplifies Eq. 1 to

$$dS/dt = -T(t) \quad (2)$$

with the scale of mass per tree per time. The assumption that soil evaporation losses are a minor component of evapotranspiration under the footprint of tree canopies during the growing season is demonstrated in studies that partition fluxes at the stand scale (Wilson et al. 2001, Oishi et al. 2008). In the absence of precipitation, soil moisture remains below field capacity, so gravitational runoff and drainage in the rooting zone are negligible (Feng et al. 2014, Dingman 2015). This model tracks total moisture and thus allows for redistribution within the rooting zone, for example through hydraulic lift or catenary subsurface flow, although we do not model these processes explicitly. To match precipitation data, the terms in a model like Eq. 1 would typically have dimensions of mm/time. One not-so-obvious consequence of shifting from Eqs. 1 to 2 is the potential it offers to translate sap flux observations to the soil reservoir, both in terms of mass per day.

The potential reservoir, $\omega_i$, is unknown and is not directly measurable for individual adult trees. However, we can assume recharge at the onset of a drought and estimate this reservoir from the trajectory of depletion. Then, the reservoir state for an individual tree during drought is the balance between the potential reservoir ($\omega_i$, kg) and transpiration ($T_{i,t}$, kg/d) summed through time

$$S_{i,t} = S_{i,t-1} - T_{i,t-1} = \omega_i - \sum_{c=0}^{t-1} T_{i,c}. \quad (3)$$

Losses for an individual tree, $i$, on day $t$ are driven by atmospheric demand from potential evapotranspiration ($\mathrm{PET}_{i,t}$, $\mathrm{kg{\cdot}m^{-2}{\cdot}d^{-1}}$), crown area ($A_i$, $\mathrm{m^2}$), and the remaining water reservoir (kg) (Kramer 1937, Kozlowski 1949). Here, we assume a constant crown area through time because our data are over relatively short time scales. Additionally, since full recharge is not guaranteed, we include an initial latent state ($T_{i,0}$) that allows for some depletion at the beginning of each drought.

Estimates of $\omega_i$ and $S_{i,t}$ require a transpiration model, suggested by the observation that sap flux declines with moisture availability (Meinzer et al. 2013). The simplest assumption is that transpiration declines are proportional to the remaining reservoir. This assumption needs testing across multiple droughts. Using this assumption with the standard transpiration dependence on potential atmospheric demand, we have a model for transpiration

$$\frac{T_{i,t}}{A_i} = \mathrm{PET}_{i,t}\frac{S_{i,t}}{\omega_i} \quad (4)$$

where $S_{i,t}/\omega_i$ is the fraction of the reservoir remaining (kg/kg). Eq. 4 specifies the reservoir effect while abstracting the features of transpiration models that represent hydraulic status and stomatal control (Whitehead 1998, Cruiziat et al. 2002, Bell et al. 2015).

To make reservoir predictions for trees that did not have transpiration observations, we modeled the natural log of the potential moisture reservoir as a linear function of the natural log of tree diameter at breast height ($D_i$), the local topographic wetness index ($W_i$, a measure of the local slope and uphill drainage area), and intercept effects for each species ($\boldsymbol{Z_i}$)

$$\ln \omega_i = \beta_0 + \beta_1 \ln D_i + \beta_2 W_i + \beta_3 W_i ln D_i + \beta_s Z_{i,s}. \quad (5)$$

We included an interaction term between diameter and the wetness index to address differences in belowground allocation with changes in the local moisture environment.

In this model, transpiration increases with demand but, as drought progresses, the depleted reservoir ($S_{i,t}/\omega_i$) increasingly limits transpiration. Combining Eqs. 3 and 4, the transpiration at a given time during a drought depends on the

cumulative losses through transpiration relative to the maximum accessible soil moisture reservoir

$$T_{i,t} = A_i \mathrm{PET}_{i,t}(1 - \omega_i^{-1} \sum_{c=0}^{t-1} T_{i,c}). \quad (6)$$

The combined effects of demand and uptake on transpiration differ between species and size classes (Cruiziat et al. 2002); trees with large exposed canopies may have high atmospheric demand, and trees with large root systems may have large reservoirs (McDowell and Allen 2015).

With this model, we can calculate multiple drought stress metrics. The vulnerable trees are those with a reservoir nearing depletion during droughts. The cumulative effect of reservoir deficit can be evaluated as missed transpiration (Denmead and Shaw 1962). For each tree and day, the fitted model provides a predictive distribution of the fraction of the moisture reservoir remaining (dimensionless)

$$R_{i,t} = 1 - \omega_i^{-1} \sum_{c=0}^{t-1} T_{i,c} \quad (7)$$

and the cumulative deficit between actual and potential transpiration (kg/m$^2$ canopy area)

$$\delta_{i,t} = \sum_{c=0}^{t} (\mathrm{PET}_{i,c} - A_i^{-1} T_{i,c}). \quad (8)$$

The remaining reservoir fraction is an indicator of the instantaneous stress experienced by a tree at a given time while the cumulative water deficit is an integrated measure of "missed" potential transpiration. Stand vulnerability is amplified when many trees approach these limits.

### *Data for model fitting*

We tracked transpiration by measuring sap flux over five years in a temperate forest stand of mixed hardwood and pine trees in the Duke Forest, Orange County, North Carolina, USA (35°59′01″ N, 79°05′36″ W, 155 m above mean sea level). The stand occupies a hillslope with loam soils from the Enon series that are similar in profile characteristics throughout. The tree species segregate along this hillslope gradient but individuals of most species are found throughout the stand. Continuous sap flux observations were collected for 76 trees from 10 species (Appendix S2: Table S1) over 5 yr (2010–2014), including eight independent moisture deficit periods that extended more than 14 d. Trees were selected to cover a range of sizes and landscape positions for each species. We identified meteorological droughts as intervals of at least 14 d when consecutive days had <5 mm of recorded precipitation that were within the core growing season at the site. These criteria coincided with periods when surface soil moisture levels were declining (Appendix S2: Fig. S1).

A large number of models provide estimates of daily PET over a vegetated surface with parameterization from local weather station data (Rao et al. 2011). We used climate data collected at the site to monitor precipitation and potential evapotranspiration and employed Penman-Monteith reference estimates of PET provided by the Remote Automated Weather Station at the site (National Interagency Fire Center, Boise, Idaho, USA). Here, PET is observed at the stand scale and we estimate the individual-level value with an observation error in the model, such that we allow for individual-tree variability in the stand-level observation of PET per canopy area. Canopy area can be approximated as the exposed surface area as viewed from above (Wyckoff and Clark 2005). We estimated the exposed canopy area of each sample tree by measuring the major and minor axes of canopy exposed to the sky and assuming an ellipsoid shape. These estimates of exposed canopy area were comparable to other approaches. They were correlated with estimates based on inverting the actual transpiration and potential transpiration for each tree under wet conditions ($r = 0.61$) as well as predictions based on tree diameter from previous observations at the site ($r = 0.78$).

We estimated transpiration rates based on measurements of sap flux density for each tree over the first 2 cm of the xylem with Granier-style thermal dissipation probes (Lu et al. 2004) that were installed on north-facing aspects of each tree at breast height (1.4 m) and shielded with reflective insulation. Observations were collected every minute and then averaged and recorded as ten-minute averages. Estimates of sap flux density were based on the empirical thermal dissipation calibration from Granier (1985). We scaled these estimates to whole-tree transpiration with empirical models that we previously developed to account for radial variation in sap flux rates based on tree size and xylem anatomy (Berdanier et al. 2016). These whole-tree transpiration estimates were integrated by day.

### *Model fitting*

We employed a Bayesian state-space modeling framework that combined our observations with Eq. 6 while accounting for the temporal dependence and uncertainty in the model (Appendix S1). The state-space approach allows us to separate the error in our whole-tree transpiration estimates, by modeling the latent actual transpiration, from the error in the temporal process of reservoir depletion. Parameters for the moisture reservoir and the latent states of transpiration were estimated with the mass balance model, where the actual transpiration at day $t$ since the onset of drought for tree $i$ in drought $d$ depends on the transpiration calculated from sap flux ($y_{i,d,t}$) and the accumulation of the actual, unobserved transpiration values ($T_{i,d,t}$) through time. Actual transpiration is a latent predicted state with a conditionally normal distribution including process error. Variance parameters were assigned inverse-gamma distributions. We specified a normally distributed error (an individual random effect) on the potential transpiration estimates to account for uncertainty in local microclimate among trees through time and to estimate the individual-level potential transpiration per canopy area.

We used Markov chain Monte Carlo (MCMC) simulation to sample from the joint posterior distribution for all model parameters. Specifically, we wrote a Metropolis-within-Gibbs algorithm (Gelfand and Smith 1990) in R version 3.2.3 (R Core Team 2015). Estimates of the latent transpiration states, potential transpiration values, regression parameters, and variance parameters were sampled directly from conditional posterior distributions. The potential moisture reservoir was sampled with a Metropolis-Hastings step. We

fit the model with 22,000 iterations, excluding the first 2,000 iterations before summarizing the posterior distribution for each parameter to ensure parameter convergence. Convergence was assessed based on MCMC acceptance criteria for each Gibbs step and visual examination of the resulting parameter traces (Appendix S2: Figs. S3, S4). All estimates of the moisture reservoirs had a potential scale reduction factor <1.1, providing evidence of convergence (Gelman and Rubin 1992). The model converged quickly due to direct sampling from the conditional posterior distributions for all parameters except for the estimates of the moisture reservoir. Code and relevant data for the model are available online (Berdanier and Clark 2017).

### *Testing the model*

A critical validation for the mass balance approach is the demonstration that it predicts the same total reservoir mass for each tree across multiple droughts and the rate of moisture depletion over time. Each drought features a unique and variable progression of atmospheric demand and individual transpiration rates. We expect the mass balance to converge to consistent estimates for the potential reservoir if individual trees effectively exploit a given soil volume that controls the rate and timing of transpiration. If the mass balance works, then inverting this relationship should track the depleting reservoir. If the model can predict the rate of depletion, then predictions should agree with next-day transpiration observations and should correlate with observations from other trees. We tested the out-of-sample predictive ability of the fitted model parameters with independent observations (not used in model fitting) from six *Pinus taeda* trees measured during a 23-d late-summer drought in 2007 near Plymouth, Washington County, North Carolina, USA (J.-C. Domec, *unpublished data*), and in-sample observations with day-ahead predictions. If the potential moisture reservoir is consistent through time then its depletion should affect performance and thus explain the individual variation in growth and fecundity in forest stands (Berdanier and Clark 2016*b*, Clark et al. 2016). We related the measures of drought stress in Eqs. 7 and 8 to independent, concurrent observations of physiological condition and demographic performance during a severe seasonal drought at the site in 2010 (Palmer Drought Severity Index = −1.9, 93rd percentile of historical observations).

*Predicting ecophysiological responses.*—First, we tested the effect of reservoir depletion on physiological damage by examining the relationship between mid-day loss of hydraulic conductance and the remaining reservoir fraction. If the reservoir fraction represents the soil moisture and water potential that a tree experiences, then we expect reservoir depletion to increase xylem tension and lead to loss of conductance. We estimated loss of hydraulic conductance with two approaches, native and rehydrated branch sample conductance ($n$ = 15) and whole tree conductance from the plant water potential gradient ($n$ = 12).

For native branch conductance, sun-exposed branches were cut during the drought and placed in black plastic bags with moist towels. Each branch sample was at least two times the length of measured xylem conduits for the given species. The samples were cut again under water before measuring native specific conductivity, rehydrating, and measuring maximum specific conductivity. The ratio of these measures is the native loss of conductance (Domec et al. 2005). Whole tree hydraulic conductance was calculated three times in 2010, before, during, and after the drought, with predawn and midday measurements of leaf water potential on trees that were monitored with sap flux sensors. At each sampling for each tree, leaf water potential was measured on two sky-exposed leaves and averaged. We calculated whole tree conductance as $K_{\text{tree}} = \frac{T}{(\psi_{\text{predawn}}) - (\psi_{\text{midday}} - 0.098\,h)}$ for each tree at each date, where $T$ is the hourly transpiration rate (kg/h) at the time when the midday leaf was sampled and $h$ is the height (m) (Wullschleger et al. 1998). Then, we estimated loss of whole tree conductance as one minus the ratio of the conductance during the drought ($K_{\text{tree}(i,d,t)}$) to the maximum observed over the three sampling dates. This water potential gradient approach incorporates the loss of conductivity in the branch and leaves, so we expect these loss of conductance estimates to be greater than those from the branches. However, consistency in the responses of whole tree and branch estimates to declines in soil water pools provide multiple lines of evidence for physiological impacts of tree water balance.

We modeled the effect of reservoir depletion on each loss of conductance measure independently with a linearized power function on the fraction of water used (or 1 – fraction remaining) with no intercept

$$\ln(k_{i,d,t}) = \alpha_K \ln(1 - R_{i,d,t}) + \varepsilon_K \tag{9}$$

where $\kappa_{i,d,t}$ is the loss of conductance measure on day $t$, $\alpha_K$ is the effect parameter, $R_{i,d,t}$ is the fraction of the remaining reservoir (Eq. 7) on the same day, and $\varepsilon_K$ is the error for the branch or the whole tree conductance ($K_{\text{branch}}$ or $K_{\text{tree}}$). The effect parameter represents the curvature of the response. In this model, when $\alpha_K$ is greater than zero, the loss of conductance is equal to one when the remaining reservoir fraction is equal to zero and it is equal to zero when the remaining reservoir fraction is equal to one. We fit the effect parameters and errors with a normally distributed Bayesian regression where $\alpha_K$ was constrained to be greater than zero. Because the observations here are sampled from individual branches and leaves, we expect variance in the data. Parameter estimates were sampled directly from conditional posterior distributions with MCMC.

*Predicting demographic impacts.*—We tested the effect of physiological stress on productivity by examining the relationship between the cumulative transpiration deficit over the drought ($\delta_i$) and the recovery of biomass growth and reproductive output after the drought. Carbon gain is maximized at full reservoir recharge when $T_{i,t}/A_i$ approaches $\text{PET}_{i,t}$ (Denmead and Shaw 1962). The cumulative difference between these terms during drought, the missed transpiration, should differ among trees and translate to growth and fecundity. Biomass and reproductive output (seed biomass) were estimated from observations at the site throughout the study period (Clark et al. 2010, Berdanier and Clark 2016*b*), and biomass growth rates were calculated by taking the difference in biomass between years. We calculated

recovery for measured trees ($n$ = 50) based on the log ratio of the rates after and before the drought for biomass growth ($G$) and reproductive output ($F$), $\gamma_i = \ln(G_{i,2011}/G_{i,2009})$ and $\lambda_i = \ln(F_{i,2011}/F_{i,2009})$ (Berdanier and Clark 2016*a*). For these ratios, positive values indicate recovery and negative values indicate a lower rate after the drought than before. We modeled the effect of transpiration deficit on recovery with a multivariate linear model

$$[\gamma_i \lambda_i] = [\alpha_g\ \alpha_f] V_i + \Sigma \quad (10)$$

where $\boldsymbol{\alpha}_g$ and $\boldsymbol{\alpha}_f$ are regression parameters for each recovery measure, $\boldsymbol{V}_i$ includes variables for an intercept and the log of transpiration deficit, ln ($\delta_i$) (Eq. 8), and $\boldsymbol{\Sigma}$ is the covariance of growth and reproductive recovery. We fit the regression parameters and error with a multivariate normally distributed Bayesian regression. Parameter estimates were sampled directly from conditional posterior distributions using MCMC.

*Predicting landscape consequences.*—Finally, we predicted moisture reservoirs from Eq. 6 and drought stress measures from Eqs. 7 and 8 for all measured trees in the stand to examine landscape patterns and test the aggregate estimates against independent measures at the landscape scale. Drought stress metrics were calculated for all trees in the stand for a 24-d mid-summer drought in 2014, chosen because it contained the largest sample of concurrently monitored trees ($n$ = 69). For the unmonitored trees in the stand that were within the ranges of the potential reservoir predictor variables ($\tilde{n}$ = 1,589), we applied the model to predict transpiration through time and generated summary statistics of reservoir depletion and cumulative transpiration deficit as above. These modeled trees comprised 74% of the basal area of the stand.

Stand reservoir depletion was calculated as the sum of the aggregated cumulative transpiration divided by the sum of the potential reservoirs across trees at each time $(\sum_{i=1}^{\tilde{n}} \omega_i)^{-1} \sum_{i=1}^{\tilde{n}} \sum_{c=0}^{t-1} T_{i,d,c}$. We compared this measure with transpiration estimates from MODIS over the site and from an eddy flux tower that was within 1 km of the site to confirm the magnitude of our landscape estimates. For both comparison values, we assumed an area-averaged potential soil reservoir with local measurements of soil water holding capacity ($m^3_{water}/m^3_{soil}$) and an estimate of soil depth (m), converted to a volume per area (mm). Estimates of potential and actual evapotranspiration from MODIS (Mu et al. 2011) and the flux tower were reported in mm over the same time interval as the tree predictions. We plotted the estimates of reservoir depletion for measured trees and the predictions for the whole stand vs. the local tree aridity index ($\omega_i^{-1} A_i \sum_{c=0}^{t-1} \mathrm{PET}_{i,d,c}$) at each time point during the drought for comparison with the hydrological Budyko curve (Budyko 1974), which shows the trajectory of reservoir depletion during drought as a function of atmospheric demand relative to soil supply.

## Results

Across different drought events, our predictions of accumulated transpiration from the model converged to consistent estimates of the potential reservoir $\omega_{i,t}$ (Appendix S2: Figs. S2, S3). Reservoir estimates differed among trees (Fig. 1) based on tree diameter ($\beta_{\ln(DBH)}$ and 95% credible interval [CI] = 4.93 [1.49, 8.37]), landscape moisture index ($\beta_{TWI}$ [95% CI] = 2.30 [0.43, 4.17]), and species-specific coefficients (Appendix S2: Table S1, Fig. S4). The reservoir estimates were less sensitive to tree diameter when the moisture index was high ($\beta_{\ln(DBH)\times TWI}$ [95% CI] = −0.68 [−1.26, −0.10]), so the effect of tree diameter was amplified in upland, dry sites. Large *Pinus* trees in these habitats were predicted to have the largest reservoirs. Estimates across trees approximate volumes of individual belowground reservoir control, ranging from 75 to over 4,600 kg of water, with an average coefficient of variation in estimates of 6% across trees. Day-ahead predictions of transpiration declines (Fig. 1b) were accurate over the range of transpiration rates observed in the study (Fig. 1b inset, shaded points, $r$ = 0.97, root mean square predictive error

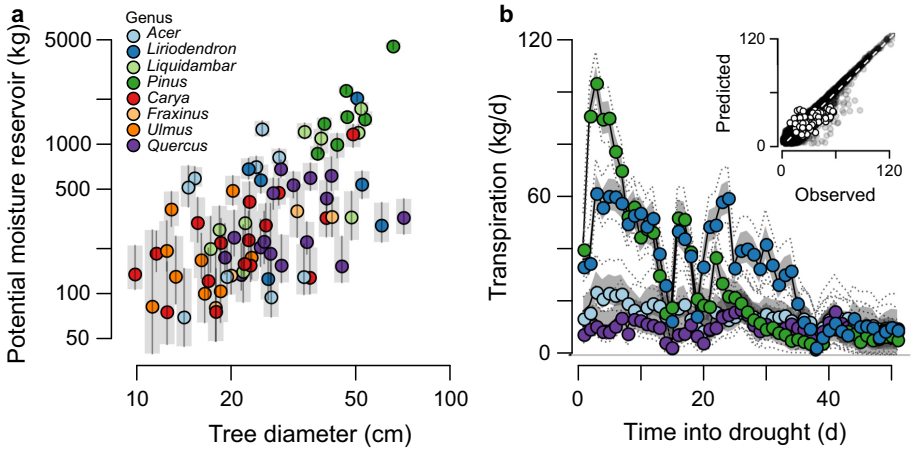


Fig. 1. Variation in tree moisture reservoirs and transpiration declines during drought. (a) Predictions (and 95% credible intervals) for the potential reservoir ($\omega_i$) across trees (colored by genus) and sizes ($D_i$). (b) Observations (points) and day-ahead predictions (gray-shaded 95% credible intervals, dotted 95% predictive interval) for four example trees during the 2010 drought. Inset shows day-ahead (shaded points) and out-of-sample (open points) predictions for observations.

[RMSPE] = 5.3 kg/d) despite substantial variation within and between trees. Additionally, the model produced good drought-response predictions for out-of-sample measurements from independent trees (Fig. 1b inset, outlined points), with an average correlation across trees of 0.68 and an average RMSPE across trees of 11.8 kg/d.

At the height of the severe seasonal drought in the summer of 2010, trees nearing reservoir depletion were those with the greatest loss of branch ($\alpha_{branch}$ [95% CI] = 3.72 [3.50, 3.93], RMSE = 0.17) and whole-tree ($\alpha_{tree}$ [95% CI] = 0.95 [0.92, 0.99], RMSE = 0.14) hydraulic conductance (Fig 2a). We found that species experienced different cumulative transpiration deficits over the 2010 drought (Fig. 2b). Trees with low cumulative deficits showed increased growth recovery following this drought relative to pre-drought levels (Fig. 2c; $\alpha_{growth}$ [95% CI] = −1.04 [−1.47, −0.60], RMSE = 0.32). Trees with high cumulative deficits showed declines in reproductive output relative to pre-drought levels (Fig. 2d; $\alpha_{fecund}$ [95% CI] = −4.26 [−6.16, −2.34], RMSE = 1.47).

At the landscape scale, we estimated a potential tree reservoir of 51 kg water per $m^2$ of surface area (Fig. 3a). Accounting for an average gravimetric soil water holding capacity of 41.1% in this stand and an average soil bulk density of 1,270 kg soil/$m^3$, our estimate of the potential moisture reservoir indicates an average potential tree reservoir depth of 9.8 cm, not including root biomass and rocks. After 24 rain-free days, predicted aggregate reservoir depletion throughout the stand (mean [95% CI] = 0.58 [0.44, 0.69]) did not significantly differ from independent estimates from MODIS and a nearby flux tower (mean [95% CI] = 0.69 [0.59, 0.79] and 0.59, respectively), providing evidence for consistency between our aggregate estimates and larger-scale observations. Predicted drought trajectories of both individual trees and the whole stand followed the hydrological Budyko curve (Appendix S2: Fig. S5). Predictions from the model suggest that trees in upland areas generally drew down their soil water resources during the drought (Fig. 3b), increasing the loss of conductance (Fig. 2a). Yet, cumulative transpiration deficits were predicted to be widespread throughout the stand (Fig. 3c), and trees in both lowland and upland environments were predicted to experience cumulative stress from reservoir depletion.

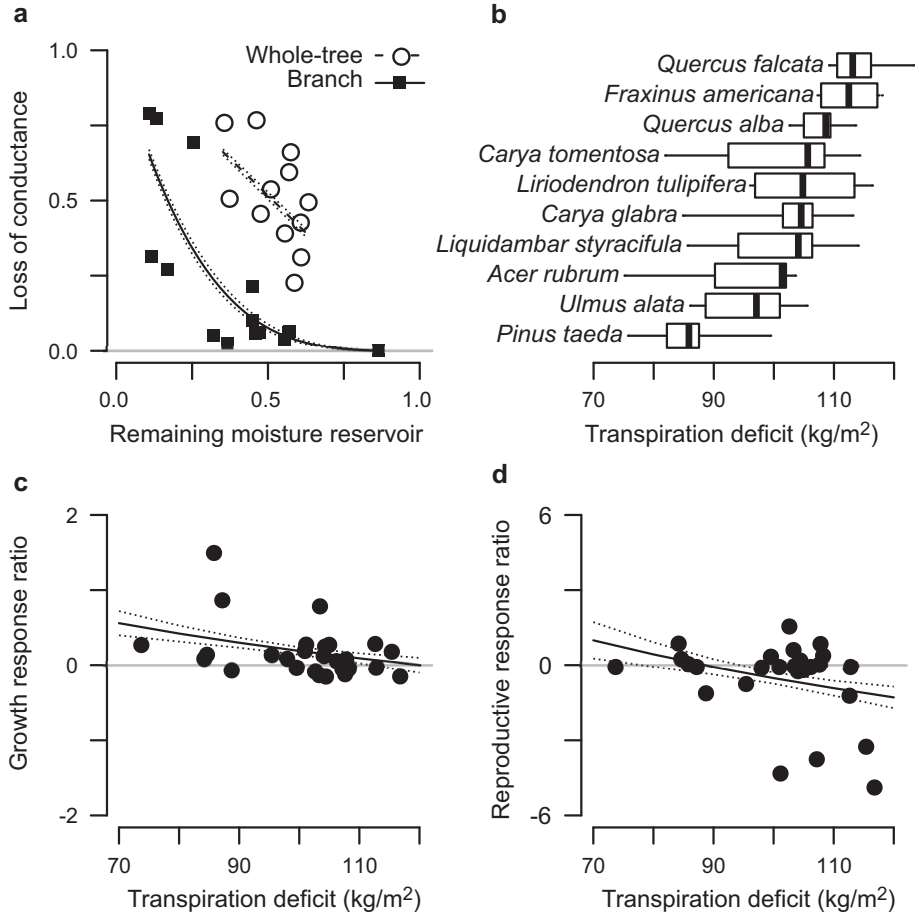


FIG. 2. Ecophysiological responses to drought. (a) Loss of branch (filled squares) and whole-tree (open circles) hydraulic conductance with declines in relative moisture reservoir (reservoir state divided by potential reservoir, $S_{i,t}/\omega_i$) during drought. (b) Species differences in transpiration deficits per canopy area. The box plot shows medians (vertical line), first and third quartiles (box), and 1.5 times the interquartile range (whisker). (c) Biomass growth response in the year after the drought ($\ln[growth_{post}/growth_{pre}]$) was greatest for trees with low cumulative transpiration deficits during the drought while (d) reproductive response ($\ln[fecundity_{post}/fecundity_{pre}]$) was lowest for trees with large cumulative transpiration deficits. Lines in each panel show fitted model predictions and confidence intervals.

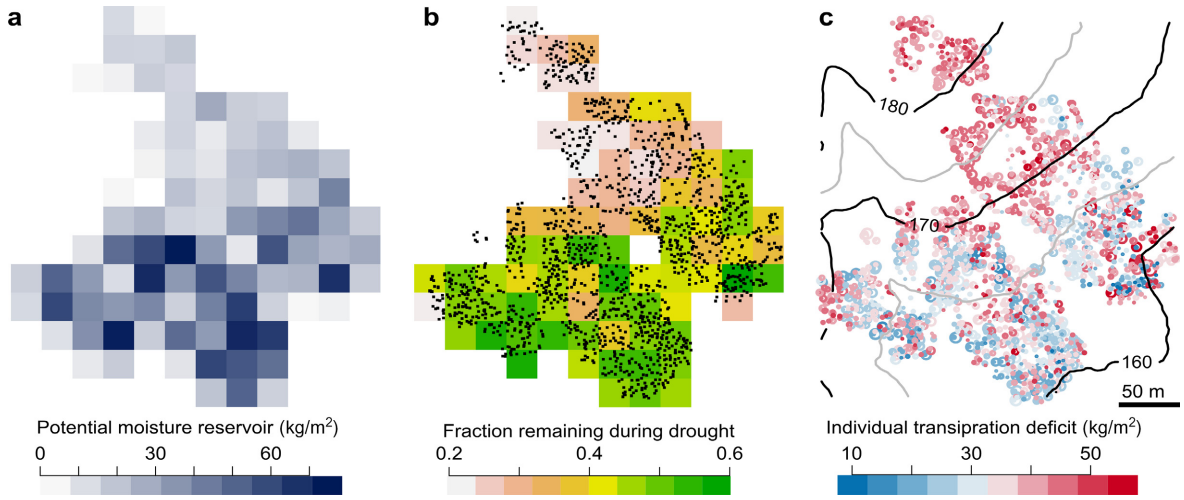


FIG. 3. Forest stand drought predictions. (a) Variation in the potential moisture reservoir available to trees throughout the stand. (b) Trees (points) in landscape positions with low moisture availability were predicted to have the largest relative reservoir depletion during a mid-summer drought in 2014. (c) Individual trees throughout the landscape showed patchy responses in predicted cumulative transpiration deficits per leaf area, depending on their water balance (circle size relative to tree diameter). Topographic contours (m above mean sea level) are shown in panel c.

## DISCUSSION

Ecologists have struggled to predict forest responses to drought because of extreme diversity of water use by trees across variable environments (Allen et al. 2015). Here, we demonstrate how tree water balance determines drought responses across sizes, species, and landscape positions. Individual drought responses are predicted by the mass balance of atmospheric demand and the moisture reservoir. With simple tree-scale measurements and a network of sap flux observations, the mass balance can be used to predict differential access to soil moisture (Hanson and Weltzin 2000), understand ecohydrological variation across forest stands (Nippgen et al. 2015), and identify trees that are vulnerable to damage from future droughts (Clark et al. 2016). The trees that control large potential moisture reservoirs can maintain transpiration during drought and avoid both short- and long-term injury after drought as long as their reservoirs are not depleted.

The mass balance approach demonstrated that the potential reservoir available to individual trees can be estimated with data across droughts over the span of a few years. The model predicts the dynamics of soil water use at the tree scale as transpiration progressively declines during drought and trees experience moisture limitation (Fig. 1). The estimates of individual moisture reservoirs are supported by out-of-sample observations that are consistent with predictions from the scale of individual trees to the whole stand. While there are differences throughout the landscape, aggregate stand-level estimates from this individual model agree with large-scale observations from MODIS and a nearby flux tower. Reliable estimates of moisture reservoirs in dense stands indicate that moisture limitation can be predicted from individual tree characteristics and suggest that it should explain tree fitness and predict vulnerability throughout the stand.

The physiological effects of drought depend on individual water balance during and after droughts. Injury in peripheral organs along with stomatal closure or leaf wilting (Sperry et al. 2002, Brodribb et al. 2003) can explain the observed and predicted declines in transpiration as the drought progressed (Fig. 1b), although we cannot disentangle these processes with the mass balance model because it does not explicitly track stomatal closure or loss of conductance. The empirical connection between whole-tree reservoir depletion and loss of conductance across organs creates new opportunities to predict whole-tree drought stress by incorporating individual differences in size and topographic position in addition to differences among species. Predictions from the mass balance model are also related to measures of demographic fitness. The declines in productivity that we observed (Fig. 2b–d) can last for years after severe droughts and set trees on a trajectory to mortality (Anderegg et al. 2015, Berdanier and Clark 2016*a*). The reservoir impact of drought thus provides the connection between short-term physiological responses and multiyear fitness.

While large trees may access a large potential moisture reservoir (Fig. 1a), they may also lose more water through transpiration during a drought. Transpiration declines depend on moisture reservoirs relative to atmospheric demand (Matheny et al. 2017). Both the moisture reservoir and the exposed canopy area are influenced by size, species, and topographic position, all of which contribute to the spatial patterns in the cumulative deficit during drought (Fig. 3). Consequently, the cumulative transpiration deficit does not necessarily decrease with increases in size.

These results highlight species differences in drought tolerance. For example, *Quercus* species generally do not access a large reservoir, meaning that their drought tolerance must be attributed to other features (Roman et al. 2015). By contrast, the regionally common *Pinus taeda* likely benefits from a remarkable capacity to dominate soil moisture (Oosting and Kramer 1946), having the largest reservoirs of all species we analyzed. Our predictions of differences in transpiration deficits across species suggest that future increases in atmospheric deficits and longer rain-free periods may

change species composition. Anticipating these stand-scale shifts relies on estimates of individual demographic performance that impact stand-level dynamics. These shifts could occur through physiological injury and the cumulative impact of missed transpiration on growth and reproduction (Fig. 2). The mass balance facilitates estimates of variables that are related to demographic performance, including reservoir depletion and transpiration deficits (Fig. 3).

The finding that reservoir capacity and depletion can be predicted from tree species, size, and topographic position provides predictive potential for drought vulnerability throughout forest stands based on measurements from a sample of trees. Patterns in drought sensitivity (Fig. 3) depend on landscape position (Gaines et al. 2016) as well as species identity (Matheny et al. 2017). While root biomass allocation decreases with increasing precipitation across sites (Mokany et al. 2006), rooting depth has been shown to be similar across xeric and mesic landscape positions within temperate forests (Gaines et al. 2016). Our landscape-level findings support these studies, with increases in the predicted moisture reservoir in mesic areas but a negative interaction with tree diameter, meaning that the reservoir benefit of growing in a mesic area is dampened by reduced gains from size. These interactions have impacts on drought sensitivity, such that large trees in xeric areas can have relatively larger belowground reservoirs (Mokany et al. 2006). Conversely, light limitation of small, suppressed trees may encourage small root systems, thus increasing risk of reservoir depletion and injury during drought even in dense, mesic areas.

These results rely on a number of assumptions and include caveats that present opportunities for future research. First, we do not explicitly represent competition for moisture between trees and our analysis does not track drought recovery following precipitation or long-term responses such as changes in belowground biomass (Berdanier and Clark 2016*a*). As such, our estimates represent a steady-state moisture reservoir under the sites' current species composition. Calibration of this model in other sites will require sap flux observations, which are still not widespread in ecological studies (but see efforts such as SAPFLUXNET; Poyatos et al. 2016). Additional predictors, such as soil type, may improve the analysis of variation in moisture reservoirs across sites. Finally, when similar measurements are available across sites, predictions from this model could be compared to field observations in areas with extensive belowground sampling or to measurements from satellites or flux towers. Despite these limitations, our analysis shows that a mass balance model can be used to predict the moisture reservoir of trees and can enhance understanding of drought responses by linking ecophysiological and demographic responses to the individual water balance.

## Acknowledgments

Funding for this research was provided by NSF (grant no. EF-1137364), the Coweeta Long Term Ecological Research Program, and the Duke University Nicholas School of the Environment. We are grateful for helpful feedback from Matthew Kwit, Chantal Reid, Bijan Seyednasrollah, Bradley Tomasek, and four anonymous reviewers. We thank J.-C. Domec, D. Y. Hollinger, and C. F. Miniat for sharing physiological and eddy covariance data.

## Literature Cited

Allen, C. D., et al. 2010. A global overview of drought and heat-induced tree mortality reveals emerging climate risks for forests. Forest Ecology and Management 259:660–684.

Allen, C. D., et al. 2015. On underestimation of global vulnerability and forest die-off from hotter drought in the Anthropocene. Ecosphere 6:129.

Anderegg, W. R. L., et al. 2015. Pervasive drought legacies in forest ecosystems and their implications for carbon cycle models. Science 349:528–532.

Bell, D. M., et al. 2015. A state-space modeling approach to estimating canopy conductance and associated uncertainties from sap flux density data. Tree Physiology 35:792–802.

Bennett, A. C., et al. 2015. Larger trees suffer most during drought in forests worldwide. Nature Plants 1:15139.

Berdanier, A. B., and J. S. Clark. 2016*a*. Multiyear drought-induced morbidity preceding tree death in southeastern U.S. forests. Ecological Applications 26:17–23.

Berdanier, A. B., and J. S. Clark. 2016*b*. Divergent reproductive allocation trade-offs with canopy exposure across tree species in temperate forests. Ecosphere 7:e01313.

Berdanier, A. B., and J. S. Clark. 2017. github.com/berdaniera/WaterBalance: Berdanier and Clark Water Balance (Version 1.0).*Zenodo*. https://doi.org/10.5281/zenodo.1048413

Berdanier, A. B., C. F. Miniat, and J. S. Clark. 2016. Predictive models for radial sap flux variation in coniferous, diffuse-porous, and ring-porous temperate trees. Tree Physiology 36:932–941.

Brodribb, T. J., N. M. Holbrook, E. J. Edwards, and M. V. Gutiérrez. 2003. Relations between stomatal closure, leaf turgor and xylem vulnerability in eight tropical dry forest trees. Plant, Cell and Environment 26:443–450.

Budyko, M. I. 1974. Climate and life. Academic Press, New York, New York, USA.

Casper, B. B., H. J. Schenk, and R. J. Jackson. 2003. Defining a plant's belowground zone of influence. Ecology 84:2313–2321.

Choat, B., et al. 2012. Global convergence in the vulnerability of forests to drought. Nature 491:752–755.

Clark, J. S., et al. 2010. High-dimensional coexistence based on individual variation: a synthesis of evidence. Ecological Monographs 80:569–608.

Clark, J. S., et al. 2016. The impacts of increasing drought on forest dynamics, structure, and biodiversity in the United States. Global Change Biology 22:2329–2352.

Cruiziat, P., H. Cochard, and T. Améglio. 2002. Hydraulic architecture of trees: main concepts and results. Annals of Forest Science 59:723–752.

Denmead, O. T., and R. H. Shaw. 1962. The availability of soil water to plants as affected by soil moisture content and meteorological conditions. Agronomy Journal 54:385–390.

Dingman, S. L. 2015. Physical hydrology. Waveland Press, Long Grove, Illinois, USA.

Domec, J.-C., M. L. Pruyn, and B. L. Gartner. 2005. Axial and radial profiles in conductivities, water storage and native embolism in trunks of young and old-growth ponderosa pine trees. Plant, Cell & Environment 28:1103–1113.

Feng, X., A. Porporato, and I. Rodriguez-Iturbe. 2014. Stochastic soil water balance under seasonal climates. Proceedings of the Royal Society A 471:20140623.

Gaines, K. P., et al. 2016. Reliance on shallow soil water in a mixed-hardwood forest in central Pennsylvania. Tree Physiology 36:444–458.

Gelfand, A. E., and A. F. M. Smith. 1990. Sampling-based approaches to calculating marginal densities. Journal of the American Statistical Association 85:398–409.

Gelman, A., and D. B. Rubin. 1992. Inference from iterative simulation using multiple sequences. Statistical Science 7:457–511.

Granier, A. 1985. Une nouvelle méthode pour la mesure du flux de sève brute dans le tronc des arbres. Annals of Forest Science 42:193–200.

Hanson, P. J., and J. F. Weltzin. 2000. Drought disturbance from climate change: response of United States forests. Science of the Total Environment 262:205–220.
Jackson, T. J., J. Schmugge, and E. T. Engman. 1996. Remote sensing applications to hydrology: soil moisture. Hydrological Sciences Journal 41:517–530.
Kozlowski, T. T. 1949. Light and water in relation to growth and competition of Piedmont forest tree species. Ecological Monographs 19:207–231.
Kramer, P. J. 1937. The relation between rate of transpiration and rate of absorption of water in plants. American Journal of Botany 24:10–15.
Lu, P., L. Urban, and P. Zhao. 2004. Granier's thermal dissipation probe (TDP) method for measuring sap flow in trees: theory and practice. Acta Botanica Sinica 46:631–646.
Matheny, A. M., et al. 2017. Contrasting strategies of hydraulic control in two codominant temperate tree species. Ecohydrology 10:e1815.
McDowell, N. G., and C. D. Allen. 2015. Darcy's law predicts widespread forest mortality under climate warming. Nature Climate Change 5:669–672.
McDowell, N. G., et al. 2011. The interdependence of mechanisms underlying climate-driven vegetation mortality. Trends in Ecology & Evolution 26:523–532.
Meinzer, F. C., et al. 1999. Partitioning of soil water among canopy trees in a seasonally dry tropical forest. Oecologia 121:293–301.
Meinzer, F. C., et al. 2013. Above- and belowground controls on water use by trees of different wood types in an eastern US deciduous forest. Tree Physiology 33:345–356.
Mokany, K., R. J. Raison, and A. S. Prokushkin. 2006. Critical analysis of root:shoot ratios in terrestrial biomes. Global Change Biology 12:84–96.
Mu, Q., M. Zhao, and S. W. Running. 2011. Improvements to a MODIS global terrestrial evapotranspiration algorithm. Remote Sensing of Environment 115:1781–1800.
Nippgen, F., B. L. McGlynn, and R. E. Emanuel. 2015. The spatial and temporal evolution of contributing areas. Water Resources Research 51:4550–4573.
Oishi, A. C., R. Oren, and P. C. Stoy. 2008. Estimating components of forest evapotranspiration: A footprint approach for scaling sap flux measurements. Agricultural and Forest Meteorology 148:1719–1732.
Oosting, H. J., and P. J. Kramer. 1946. Water and light in relation to pine reproduction. Ecology 27:47–53.
Oren, R., B. E. Ewers, P. Todd, N. Phillips, and G. Katul. 1998. Water balance delineates the soil layer in which moisture affects canopy conductance. Ecological Applications 8:900–1002.
Poyatos, R., et al. 2016. SAPFLUXNET: towards a global database of sap flow measurements. Tree Physiology 36:1449–1455.
R Core Team. 2015. R: A language and environment for statistical computing. R Foundation for Statistical Computing, Vienna, Austria.
Rao, L. Y., G. Sun, C. R. Ford, and J. M. Vose. 2011. Modeling potential evapotranspiration of two forested watersheds in the southern Appalachians. American Society of Agricultural and Biological Engineers 54:2067–2078.
Richter, D. de. B., and S. A. Billings. 2015. 'One physical system': Tansley's ecosystem as Earth's critical zone. New Phytologist 206:900–912.
Roman, D. T., et al. 2015. The role of isohydric and anisohydric species in determining ecosystem-scale response to severe drought. Oecologia 179:641–654.
Sperry, J. S., U. G. Hacke, R. Oren, and J. P. Comstock. 2002. Water deficits and hydraulic limits to leaf water supply. Plant, Cell and Environment 25:251–263.
Stahl, C., et al. 2013. Depth of soil water uptake by tropical forest trees during dry periods: does tree dimension matter? Oecologia 173:1191–1201.
Vose, J. M., et al. 2016. Ecohydrological implications of drought for forests in the United States. Forest Ecology and Management 380:335–345.
Whitehead, D. 1998. Regulation of stomatal conductance and transpiration in forest canopies. Tree Physiology 18:633–644.
Wilson, K. B., P. J. Hanson, P. J. Mulholland, D. D. Baldocchi, and S. D. Wullschleger. 2001. A comparison of methods for determining forest evapotranspiration and its components: sap-flow, soil water budget, eddy covariance and catchment water balance. Agricultural and Forest Meteorology 106:153–168.
Wullschleger, S. D., F. C. Meinzer, and R. A. Vertessy. 1998. A review of whole-plant water use studies in trees. Tree Physiology 18:499–512.
Wyckoff, P. H., and J. S. Clark. 2005. Tree growth prediction using size and exposed crown area. Canadian Journal of Forest Research 35:13–20.

## Supporting Information

Additional supporting information may be found in the online version of this article at http://onlinelibrary.wiley.com/doi/10.1002/ecy.2499/suppinfo

## Data Availability

Code and data for the moisture reservoir model are available from GitHub: https://doi.org/10.5281/zenodo.1048413.